

Synthesis, Spectroscopic Characterizations, Antimicrobial, Anticancer & Anitoxidant Activities, Molecular Docking and DFT Calculations of Noval Zinc (II) Complex of 2-(Benzoylamino)-3-Sulfanylpropanoic Acid

Mohseen Ahmed, Reema Chand, Bibhesh K. Singh



Abstract: The complex with zinc (II) of Ligand (2-(benzoylamino)-3-sulfanylpropanoic) acid was made and analyzed using FT-IR, UV-visible, mass spectrometry, ¹H NMR, ¹³C NMR, SEM and powder XRD. DFT calculations were also used to detect the electronic properties & structural stability. The antimicrobial investigation demonstrated that the zinc (II) complex had better bacterial killing action against E. coli (MIC: zinc (II) complex > Ciprofloxacin > Ligand) and antifungal action against A. niger (MIC: zinc (II) complex > Ligand > Amphotericin B). And the Zn (II) complex was more antioxidant active than the free ligand in the DPPH assay, as evidenced by its lower IC 50 (~420 0). Molecular docking experiments have indicated a better binding affinity of the zinc (II) complex with major antioxidant, antimicrobial, and enzyme inhibitory proteins compared to the free ligand. The anticancer effect of the Zn (II) complex on MCF-7 cells was demonstrated to be stronger than that of the free ligand in the MTT assay, revealing that the Zn (II) complex is suitable for further development as a drug. Docking of 3D ribbon structures was used to confirm these interactions. The improved stability and electronic features of the complex, due to zinc coordination, explain the increase in its activity.

Keywords: Metal Amide Complexes, Amino Acids, Molecular Modelling, Molecular Docking, DFT, Spectroscopic Analysis, Antimicrobial Activities.

Nomenclature:

DFT: Density Functional Theorem, DMF: N-Dimethylformamide, DMSO: Dimethyl Sulfoxide, SCF: Self-Consistent Field, PDB: Protein Data Bank.

SEM: Scanning Electron Microscopy

XRD: X-Ray Diffraction

FMO: Frontier Molecular Orbital

Manuscript received on 22 August 2025 | Revised Manuscript received on 03 October 2025 | Manuscript Accepted on 15 October 2025 | Manuscript published on 30 October 2025.

*Correspondence Author(s)

Mohseen Ahmed*, Scholar, Department of Chemistry, M.B. Govt. P.G College, Haldwani, Nainital (Uttarakhand), India. Email ID: mohseenphd@gmail.com, ORCID ID: 0000-0003-3695-0692

Reema Chand, Scholar, Department of Chemistry, M.B. Govt. P.G College, Haldwani, Nainital (Uttarakhand), India. Email ID: reemachand292@gmail.com, ORCID ID: 00000-0003-0034-6178

Prof. Bibbesh K. Singh, Department of Chemistry, Govt. Degree College, Nandasain, Chamoli (Uttarakhand), India. Email ID: bibbeshksingh@yahoo.co.in, ORCID ID: 0009-0006-4186-1474

© The Authors. Published by Lattice Science Publication (LSP). This is an <u>open-access</u> article under the CC-BY-NC-ND license http://creativecommons.org/licenses/by-nc-nd/4.0/

MIC: Minimum Inhibitory Concentration DFT: Density Functional Theory MEP: Molecular Electrostatic Potential

I. INTRODUCTION

The application of transition metal complexes has become of paramount importance in recent years due to their multiple biological and chemical characteristics, which render them the most desirable drug and therapeutic agents [1]. Zinc (II) is preferred among the transition metals due to its biocompatibility, low toxicity, and key role in various biological activities, such as enzyme catalysis, DNA synthesis, and regulation of immune response [2]. Zinc has the capacity to interact with sulfur, oxygen and nitrogen donor groups in ligands that further form stable complexes with increased biological activity [3]. Such complexes are frequently more soluble, bioavailable, and reactive than the parent ligands, making them of interest to medicinal chemistry [4]. In this case, the bidentate ligand, which includes thiol and amide functional groups, was chosen 2-(benzoylamino)-3-sulfanylpropanoic acid, which allows forming strong complexes with zinc (II) [5]. This ligand not only provides a wide range of coordination opportunities but also exhibits biological activity, which can be significantly enhanced when complexed with zinc [6]. To determine the structure of the synthesized zinc (II) complex and its electronic characteristics, a set of spectroscopic and analytical methods was used, such as FT-IR, UV-visible spectroscopy, mass spectrometry, ¹H NMR and ¹³C NMR [7]. The morphological and crystalline characteristics were additionally examined with the help of scanning electron microscopy (SEM) and powder X-ray diffraction (XRD). In contrast, density functional theory (DFT) calculations [8] were used to provide insights into the geometry optimisation of the complex, the electronic distribution, and its stability [9]. The antimicrobial activity of the ligand and its zinc (II) complex was estimated using tests on bacterial (E. coli) and fungal (A. niger) strains [10]. The results of the minimum inhibitory concentration (MIC) showed that the zinc (II) complex performed better than the free ligand and wellknown drugs such as Ciprofloxacin (E. coli) and

Amphotericin B (A. niger) [11]. The molecular docking research also revealed that the zinc (II) complex presents



high binding affinities with most biological proteins, indicating that it could be better as an antimicrobial and therapeutic agent [12].

II. EXPERIMENTAL

A. Materials and Instruments

Cysteine (98%), benzoyl chloride, hydrochloric acid, methanol, ammonia, and zinc chloride (ZnCl₂, 98%) were purchased from Sigma-Aldrich and not further purified. The analysis of the elements was carried out with the help of a PerkinElmer 2400 analyzer. The **SHIMADZU** spectrophotometer 400S (400 MHz) was used to record FT-IR spectra using KBr pellets. The modified Gouy method was used to measure magnetic susceptibility at room temperature using Hg [Co (SCN)₄] as the standard. The melting points have been measured with open glass capillaries using an electrical device. ¹H and ¹³C NMR spectra were measured in DMSO-d₆ with TMS serving as an internal standard in a JEOL JNM-ECZ-400S (400 MHz). Mass spectra were taken on an Agilent Q-TOF LC/MS 6530, and UV spectra at 900 nm were taken using a LabIndia UV3092 spectrophotometer (200-900 nm). SHIMADZU DTG-60 DTA-TG (25-1000 °C) was used to test the thermal behaviour under nitrogen at heating rates of 10° C/min, the patterns of the XRD were recorded in Rigaku Miniflex system ($2\theta = 0-80^{\circ}$) using Cu K α radiation and the data was analyzed with the use of Xpert High score Plus. DFT computations were done with the Gaussian 09 B3LYP functional, LANL2DZ as the metal atoms, and 6-31G (d, p) as non-metal atoms, and the FMO and MESP surfaces were plotted by Gauss View 6. Auto Dock Vina was utilised to investigate molecular docking interactions with the selected biological targets.

B. Synthesis of Ligand

Benzamide reacted with cysteine in a 1:1 molar ratio to produce the Ligand. The benzoyl chloride was prepared by converting benzamide into benzoyl chloride using thionyl chloride (SOCl₂) in a basic solution. This activated intermediate was next slowly dropped to a cysteine solution under continuous stirring, which favoured a nucleophilic substitution. The reaction was then diluted, and acid was added after 10 minutes to precipitate the product of Scheme 1. Ligand crystals were obtained by precipitating, washing and recrystallising the precipitate. The real yield was 2.90 g of theoretical 3.63 g, representing approximately 80% yield.

[Scheme 1: Synthesis of Ligand]

C. Synthesis of Metal Complex

The zinc (II) complex of the Ligand was made by the reaction of zinc chloride and the ligand in a 1:2 molar ratio. The two were placed in a 10 per cent sodium hydroxide solution, stirred, and then refluxed at 80 °C for an additional hour to complete the complexation. After cooling, the complex was precipitated, filtered, washed and recrystallized, to give pure crystals, illustrated in scheme-2. The real yield was 5.47g, resulting in an 82% yield.

[Scheme 2: Synthesis of Zn (II) Metal Complex]

III. RESULT & DISCUSSION

The compounds which are synthesised (Schemes 1 and 2) are non-hygroscopic and crystalline. It is neither soluble in water nor soluble in ethanol, methanol, DMF or DMSO. The identity and composition of the products formed were determined by spectroscopic analysis (IR, UV-Vis, ¹H and ¹³C NMR, TOF-MS), scanning electron microscopy (SEM), Antimicrobial analysis, DFT calculations, and Molecular Docking. Analytical data and electronic spectral data of both ligand and metal complex were of 1:2 metal to ligand stoichiometry.

A. Spectroscopic Studies

i. FT-IR Spectrocopy

The FT-IR analysis of the ligand and the zinc (II) complex is used to verify the changes in coordination and bonding on complexation. The C=O band of the amide is changed to 1640 cm⁻¹ instead of 1660 cm⁻¹, and the OH bond of the ligand changes to 3350 cm⁻¹ rather than 3450 cm^{-1,} as shown in fig 1, indicating the presence of hydrogen bonding and coordination through nitrogen [13]. The fact that the carboxylic C=O peak changed to 1720-1700 cm-1, as shown in Table 1, suggests that the covalent bonding is through deprotonated oxygen. The shift in CN and NH bands proves the presence of nitrogen. The S-H and C-S interactions are also modified to indicate secondary sulphur interactions. The new bands 498, 510 and 530 cm⁻¹ represent the M -N, M -O and O -M -N vibrations and confirm the coordination of the metal to nitrogen and oxygen atoms [14].





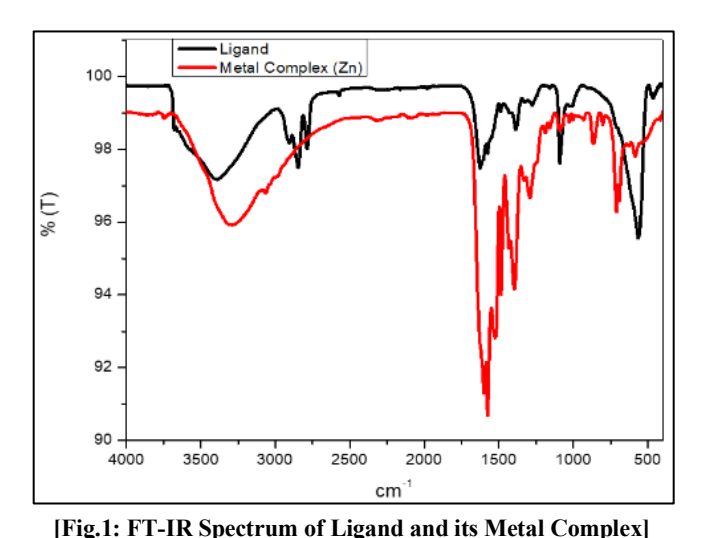


Table I: FT-IR Data of Ligand & its Metal Complex

Frequency	Ligand	Complex
ν(OH) _{Carboxylic acid}	3450	3350
ν (CO) _{Amide}	1660	1640
ν (CO) _{Carboxylic acid}	1720	1700
ν (C-N) Amide	1280	1250
ν (N-H) Amide	1540	1510
ν (-S-H)	2580	2540
ν (C-S)	680	660
ν (M-N)	-	498
ν (M-O)	-	510
ν (O-M-O)	-	530

ii. UV-Vis Spectroscopy

UV- Vis spectral spectroscopy of the Ligand and its complex reveals the presence of the $\pi 3$ - $\pi 9$ transitions in the aromatic and benzoyl systems, which lead to the Ligand absorbing at 217 and 238 nm, and the presence

of the electron-pair-pair transitions at 279 nm [15] (n) to 286 nm (p) (fig 2) in the complex. These bands shift to 215, 268, and 324 nm on complexation, with a slight shift of the 215 nm band, which remains $\pi \to \pi$ *. After the amide nitrogen and carboxyl oxygen to Zn (II) are bound, the 268 nm band $(n\to\pi^*)$ shifts [16]. The confirmation of the strong ligand-metal interaction is the ligand to metal charge transfer (LMCT) of a new band at 324 nm. Due to the d10 structure of the Zn (II), there are no d-d transitions recorded. Such spectrum properties indicate that the zinc (II) complex is tetrahedrally geometrized [17]. Fig. 2 shows the Vis spectrum of both the ligand and metal complex, and Table 2 shows the UV-Vis spectral data of the ligand and its metal complex.

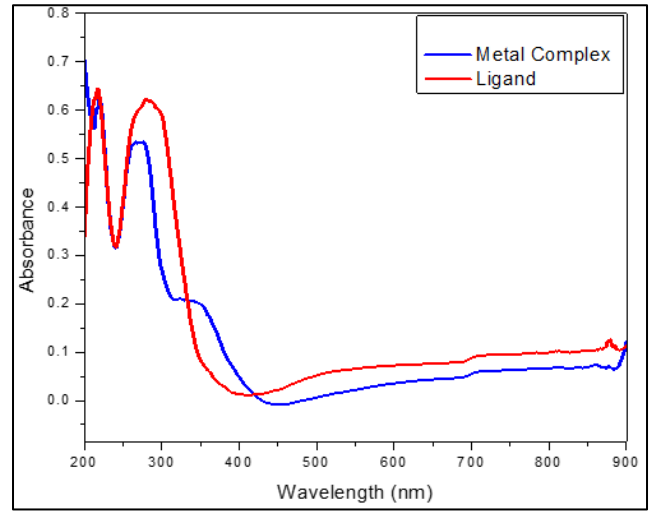


[Fig.2: UV- Vis Spectra of Ligand and its Metal Complex]

Table II: UV-Vis Spectral Data of Ligand & its Metal Complex

S.N.	Compound	Absorption	v(cm ⁻¹)	Assignment	μeff (B.M)	Proposed Geometry	
1	Ligand	217,238 279	46038, 42017 35842	π- π* n- π*	-	-	
2	Complex	215,268 324	46511, 37313 30864	n- π* LMCT	Diamagnetic	Tetrahedral	

iii. NMR Spectroscopy

Retrieval Number: 100.1/ijac.B203205021025

Journal Website: www.ijac.latticescipub.com

DOI: 10.54105/ijac.B2032.05021025

The structure of the Ligand is verified with the help of the ¹H NMR spectrum with separate proton signals [18]. The deshielded carboxylic acid proton appears at 11.89 ppm, while the amide NH proton is observed at 8.51 ppm. Both are affected by hydrogen bonding and the neighbouring carbonyl proton. The presence of aromatic protons at 7.82, 7.53, and 7.41 ppm, as shown in Fig. 3a, also indicates the environment of a benzene ring. One can find the chiral CH proton at 4.31 ppm and the diastereotopic CH₂ protons at 3.15 and 2.91ppm. The presence of the thiol group is proven by a clear SH proton signal at 2.86 ppm. The solvent, methanol, gives the peaks of 4.66 ppm (CH₃) and 3.40 ppm (OH). When it is complexed with Zn (II), the NH proton shifts to 8.01 ppm, and the aromatic protons are slightly downfielded to 4.65 ppm, 3.09 ppm, and 3.03 ppm, as shown in Fig. 3b, respectively. SH proton also changes to 2.95 ppm, which is an indication of its retention after the coordination, whereas the methanol peaks are not affected [19].

The structure of the Ligand is further confirmed using the ¹³C NMR spectrum, which has characteristic carbon signals. Carboxylic acid carbon resonates at 175.1 ppm, and the carbon (CONH) of amide is found at 167.1 ppm, indicating their deficiency in electrons. Aromatic carbons are observed at 134.3, 131.7, 128.3, and 127.4 ppm, shown in Fig. 3c, which are in agreement with a substituted benzene ring. The chiral CH carbon has a signal of 55.7 ppm, with the CH₂ carbon adjacent to the thiol group showing a signal of 29.8. At 50.1ppm, a methanol carbon (CH₃) signal is observed. All these signals change with the coordination in the zinc (II) complex, with the carboxylic carbon moving to 176.2 ppm and the amide carbon moving to 169.5 ppm, as shown in Fig. 3d. This indicates that the oxygen and nitrogen atoms coordinate the signals, respectively. Aromatic carbons exhibit more minor downfield shifts. The CH and CH2

carbons move to 62.9 ppm and 28.6 ppm, respectively, demonstrating the effect



Pub 19 Latt

Synthesis, Spectroscopic Characterizations, Antimicrobial, Anticancer & Anitoxidant Activities, Molecular Docking and DFT Calculations of Noval Zinc (II) Complex of 2-(Benzoylamino)-3-Sulfanylpropanoic Acid

of interaction with the metal-ligand. Methanol peaks are not affected [20].

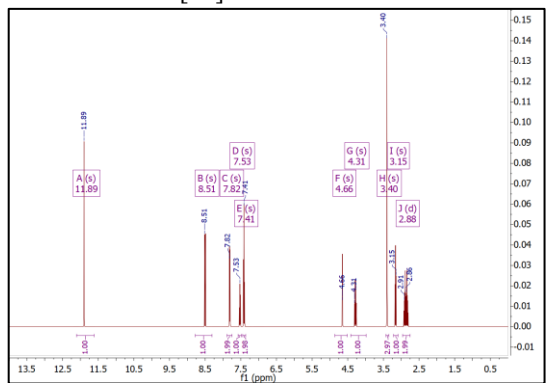


[Fig.3a: 1HNMR of Ligand]

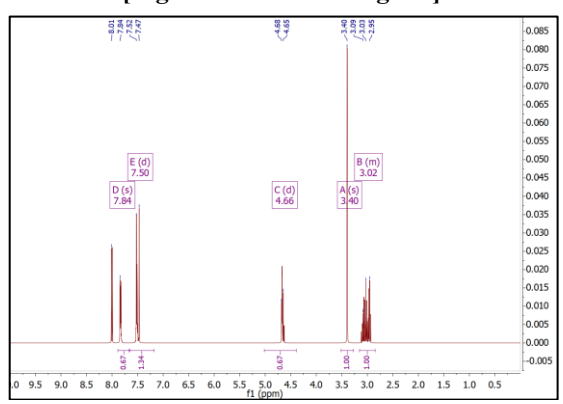


[Fig.3b: 1HNMR of Meta Complex]

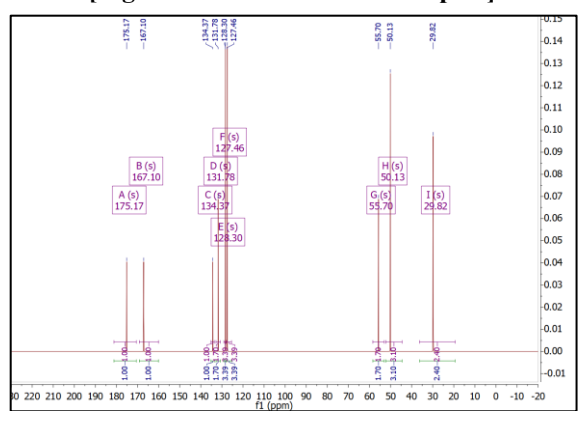


[Fig.3c: 13CNMR of Ligand]

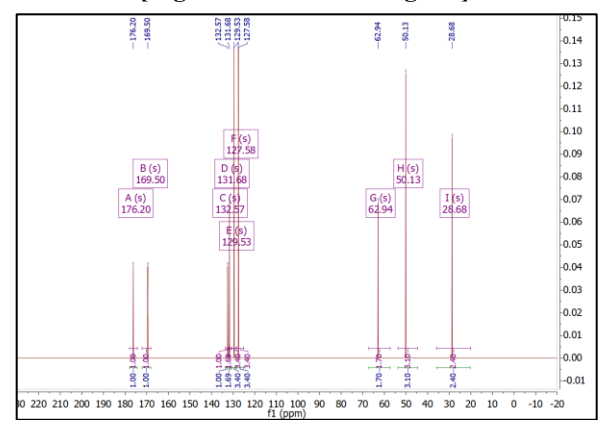


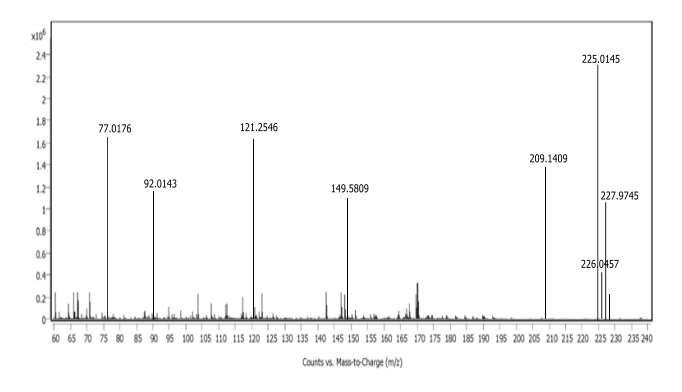
[Fig.3d: 13CNMR of Meta Complex]

iv. Mass Spectrometry

The mass spectrometric analysis of the Ligand and its zinc (II) complex can be used to give meaningful

information about the structural characteristics of the two and their fragmentation patterns [21]. The ligand has a molecular ion peak of m/z 225, which displays the intact molecular structure and isotopic peaks of m/z 226 and m/z 227 that represent natural variations in the isotopes. Notable high fragmentation intensities mainly occur at m/z 77, 92, 121,149, and 209, which indicate the location of the cleavages within the molecule. Markedly, the m/z 92 and m/z 121 peaks are related to the formation of stable aromatic fragments [C₆H₄O] ⁺ and $[C_7H_5O_2]^+$ using the benzoyl moiety, respectively. The lignad Lignad fragments into multiple masses to produce a kind of fragmentation as shown in Scheme 3, and the mass spectra of the fragmentation are given in Fig. 4a. In the zinc (II) metal complex, the molecular ion peak appears at m/z 513, which confirms the successful linkage of the ligand. Zn isotopic distribution is observed in the ions that occur at m/z 514 and m/z 515 (See Fig. 4b). The highest fragmentation is at m/z 92, 121, 225, 303, 408, and 447, indicating different dissociation of the ligandmetal. The peaks at m/z 225 and m/z 303 are the fragments of the ligand, whereas m/z 408 and m/z 447 are the fragments of the coordination sphere dissociation and rearrangement. Scheme 3: shows Mass fragmentation of the Ligand, Fig. 4a- shows Mass spectrum of Ligand and Fig. 4 b, shows Mass spectrum of Metal complex.

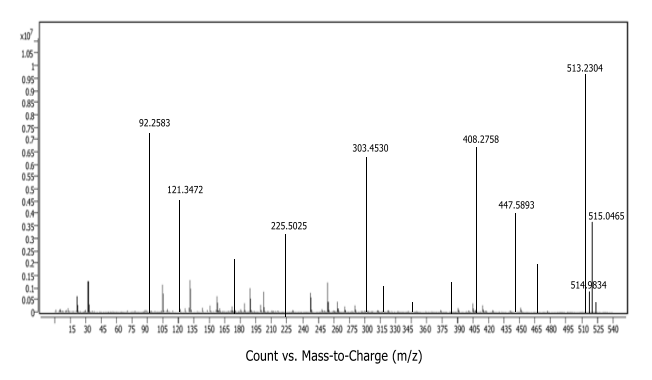
[Scheme 3: Mass Fragmentation of the Ligand]



[Fig.4a- Mass Spectrum of Ligand]



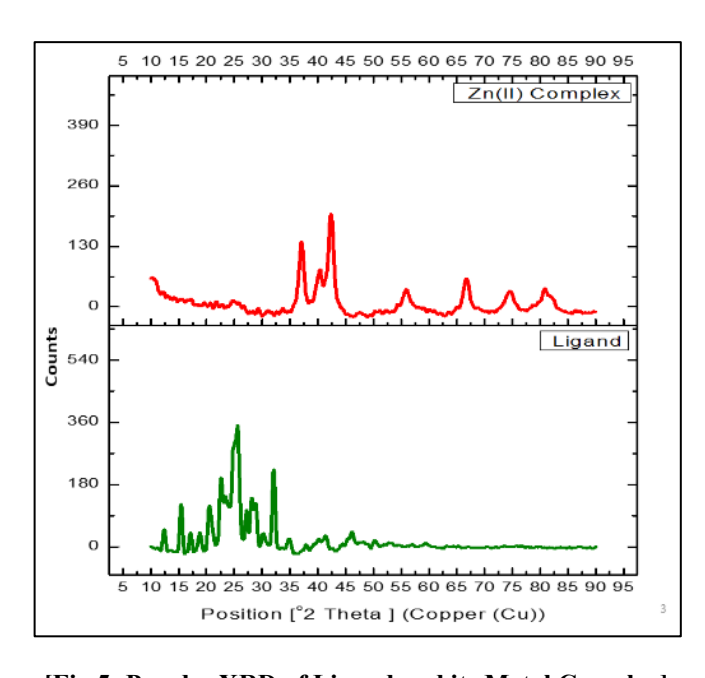




[Fig.4b: Mass Spectrum of Metal Complex]

B. Powder XRD

The X-ray diffraction of the Ligand and its complex with zinc (II) was performed with the X-ray diffractometer with the range of the diffraction angle, 2θ ranging from 0 to 90° , as shown in (Fig. 5). The XRD data of the Ligand and the zinc (II) complex has many diffraction peaks, which indicate the existence of a crystalline phase [22]. The diffraction peaks indicate that the Ligand crystal system is orthorhombic, while the zinc (II) complex crystal system is monoclinic, as confirmed by the obtained results. The tentative lattice parameters (a, b, c, α , β , and γ), inter-plane spacing (d), Miller indices (h k l) and average crystalline size of the Ligand and its zinc(II) complex are determined using a systematic trial and error strategy to optimize the fit between observed and calculated values using X'PertHigh Score Plus software as described in Each complex possess To determine the average crystallite size (D) of the zinc(II) complex and the Ligand, the Debye-Scherrer Equation was used which was $D = 0.9\lambda\beta\cos\theta$. The X-rays have a wavelength of 1.5406 Å Cu Kα [23]. The average crystallite size of the Ligand was determined to be 25.86 nm, which is lower than the 98.45 nm size of the zinc (II) complex, as shown in Table 3.



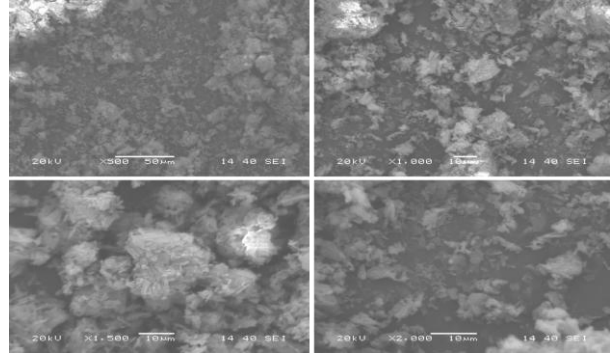
[Fig.5: Powder XRD of Ligand and its Metal Complex]

Table III: Powder XRD Spectral Data of Ligand & its Metal Complex

Empirical Formula	Ligand [C ₁₀ H ₁₀ NO ₃ S]	Zn (II) Complex [C ₂₀ H ₂₀ N ₂ O ₆ S ₂ Zn]	
Formula weight	225.00	513.00	
Temperature(K)	298	298	
wavelength (Å)	1.54	1.54	
Crystal system	Orthorhombic	Monoclinic	
Space group	Pbca	C2/c	
	a=5.6000	a=14.4310	
Unit cell dimensions	b=18.4530	b=5.3400	
Unit cen dimensions	c=14.8120	c=10.9810	
	$\alpha = \beta = \Upsilon = 90$	α=Υ=90; β=99°	
volume(A3)	1530.62	833.66	
2θ range	0-90°	0-90°	
Limiting indices	0 <h<2, 0<k<8,="" 0<l<6<="" td=""><td colspan="2" rowspan="3">0<h<7, 0<k<2,="" 0<l<5<br="">1.75 4.00</h<7,></td></h<2,>	0 <h<7, 0<k<2,="" 0<l<5<br="">1.75 4.00</h<7,>	
Density(g/cm ³)	1.47		
Z	8.00		
Particle size(nm)	25.86	98.45	
CCDC	00-039-1667	00-033-1464	

C. Scanning Electron Microscope Analysis (SEM)

The Ligand and the zinc (II) complex of the Ligand demonstrate significant structural and morphological characteristics in the SEM analysis. At low magnification (500x), their surfaces are rough, amorphous, and rock-like (fig 6a & 6b), and aggregated. With a higher magnification (1000x-1500x), a more fibrous texture and irregular clumps are observed, and hence partial crystallinity at the expense of an amorphous matrix [24]. Mixed amorphous and crystalline regions are more definite in the highest magnification (2000x), with a particle size ranging between nanometers and micrometres. Such a mixed morphology indicates increased reactivity and better metal ion-binding capabilities, which means that the Zn (II) complex is suitable for use in coordination-based applications [25].



[Fig.6a: Scanning Electron Micrograph (SEM) of Ligand]

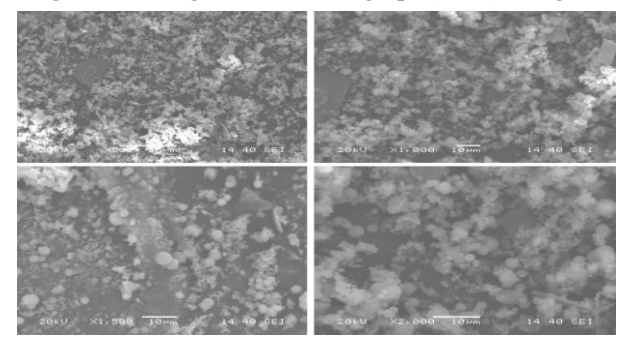


[Fig.6b: Scanning Electron Micrograph (SEM) of Metal Complex]



IV. MOLECULAR MODELING / DFT CALCULATIONS

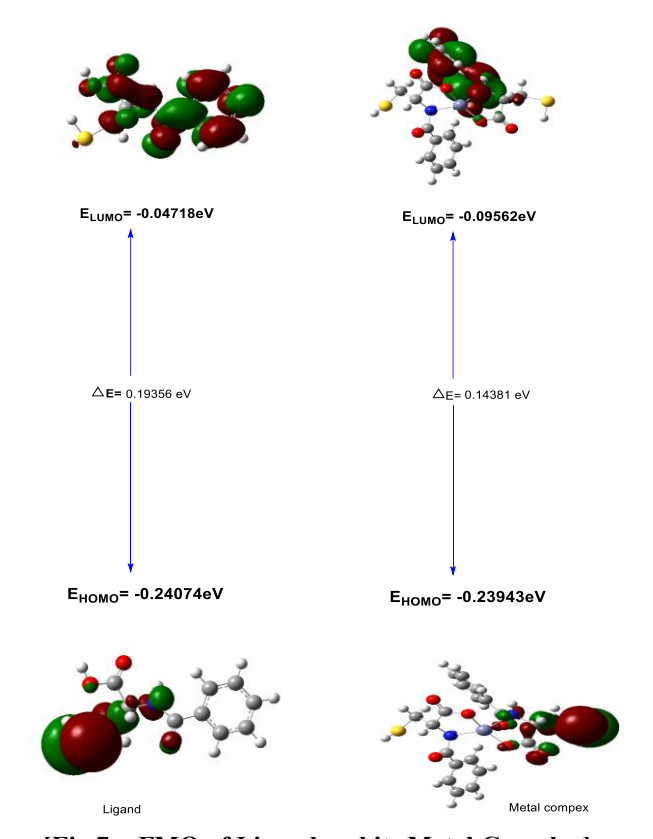
The Ligand and its zinc (II) complex were optimized using Density Functional Theory (DFT) at the RBLYP level [26]. Calculations employed the 6-31G**(d,p) and 6-311G**(d,p) basis sets for light atoms (C, H, N, O, S), and the LANL2DZ pseudopotential for the Zn metal centre to account for relativistic effects and core-electron interactions. The Ligand optimized structure (shown in fig. S9), has an energy of -29010.21 ev, an RMS gradient norm of -0.0001632 ev/Bohr, a dipole moment of 4.431163 Debye, and belongs to the C1 point group. The zinc (II) complex showed an energy of -106402.44 eV, an RMS gradient norm of -0.00010885 eV/Bohr, and a dipole moment of 7.006851 Debye. It also belongs to the C1 point group, reflecting the asymmetric nature of both systems. The essential bond lengths and bond angles are shown in Table 4. The absence of imaginary frequencies confirms both structures as true minima. These results provide insights into the strong coordination interactions between the ligand donor atoms (O and N) and Zn(II), offering significant implications for their biochemical and structural properties [27].

Table IV: Optimized Structures Bond Length & Bond Angles

Compound	Bond	Bond Length (Å)	Angle	Bond Angle(θ)
Ligand	O ₄₄ -C ₃₂ Zn ₄₇ -N ₂₄ Zn ₄₇ -O ₄₂ C ₃₂ -O ₄₃ N ₂₄ -C ₂₀ Zn ₄₇ -O ₄₂ O ₄₂ -C ₃₁ C ₃₁ -O ₄₁ N ₂₃ -C ₂₇ C ₃₀ -S ₄₅ C ₁₉ -O ₂₀ Zn ₄₇ -N ₂₃	1.3330 2.140 1.847 1.240 1.462 1.859 1.333 1.239 1.507 1.899 1.252 2.285	$Zn_{47}\text{-}N_{24}\text{-}C_{20}\\ O_{44}\text{-}C_{32}\text{-}O_{43}\\ Zn_{47}\text{-}N_{24}\text{-}C_{28}\\ O_{42}\text{-}C_{31}\text{-}O_{41}\\ C_{28}\text{-}C_{29}\text{-}O_{41}\\ N_{23}\text{-}Zn_{47}\text{-}O_{42}\\ O_{42}\text{-}C_{31}\text{-}O_{41}\\ C_{20}\text{-}C_{12}\text{-}C_{13}\\ C_{11}\text{-}C_{10}\text{-}C_{15}\\ O_{21}\text{-}C_{19}\text{-}N_{23}$	106.262 124.823 104.540 124.484 114.523 83.9087 124.484 55.291 119.991 119.505
Complex	$\begin{array}{c} N_{14}\text{-}C_{10} \\ N_{14}\text{-}C_{12} \\ C_{12}\text{-}O_{13} \\ C_{12}\text{-}C_4 \\ C_{16}\text{-}C_{18} \\ C_{18}\text{-}O_{20} \\ C_{18}\text{-}O_{19} \\ C_4\text{-}C_3 \\ C_5\text{-}C_6 \end{array}$	1.460 1.370 1.258 1.495 1.510 1.370 1.236 1.406 1.396	$\begin{array}{c} N_{14}\text{-}C_{16}\text{-}C_{18} \\ O_{20}\text{-}C_{18}\text{-}O_{19} \\ N_{14}\text{-}C_{12}\text{-}O_{13} \\ N_{14}\text{-}C_{12}\text{-}C_{4} \\ C_{4}\text{-}C_{3}\text{-}C_{2} \\ C_{16}\text{-}C_{22}\text{-}S_{25} \end{array}$	106.269 122.189 120.686 117.498 120.20 115.732

A. Frontier Molecular Orbitals (FMO) and Molecular Electrostatic Potential (MEP)

Frontier Molecular Orbital (FMO) analysis shows that the HOMO-LUMO gap of the Ligand is 0.19356 eV, shown in Fig. 7a, whereas that of the zinc (II) complex is smaller at 0.14381 eV, shown in Fig. 7 b, which means that the complex is more reactive, but less stable than the Ligand. The study of Molecular Electrostatic Potential (MEP) shows regions of electron concentration (red) and electron-deficiency (blue), whereas the Ligand has a broader distribution of charge density. The redistribution of electrons on the zinc (II) complex occurs because of coordination, and proves that the Ligand binds to the metal effectively and affects its electronic properties and reactivity [28].



[Fig.7a: FMO of Ligand and its Metal Complex]

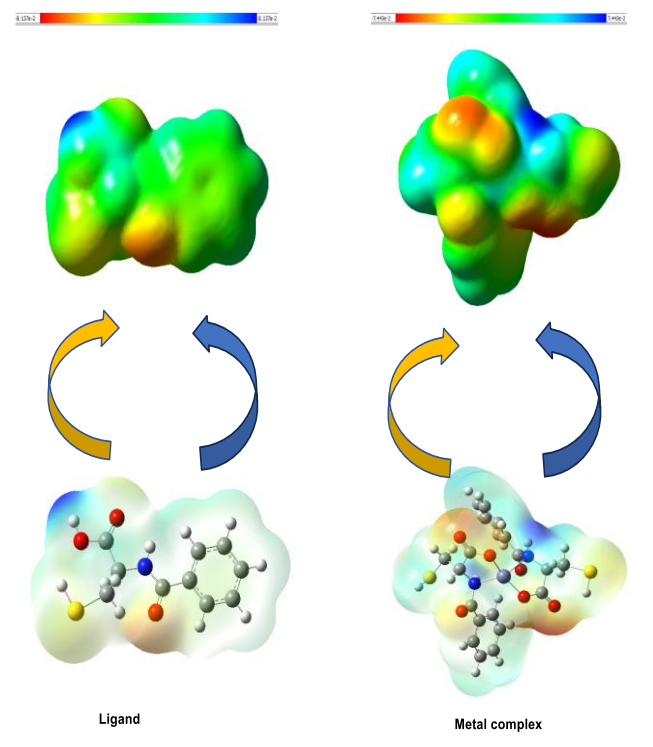


[Fig.7b: MEP of Ligand and its Metal Complex]

B. Total SCF Density

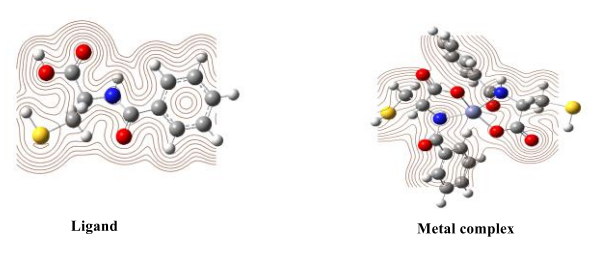
The SCF electron density analysis represents the arrangement of the electron density of the ligand and its complex with Zn (II). Oxygen, nitrogen and sulfur atoms are seen to be highly densely populated in the ligand, which

suggests metal coordination points of the ligand shown in Fig. 7c. When interacting with Zn (II), there is a





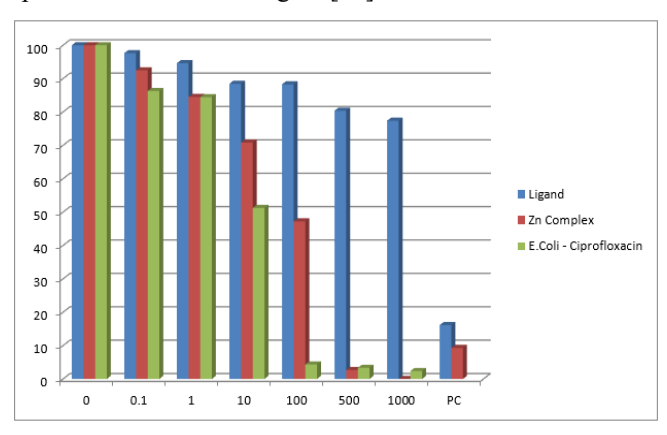
redistribution of electron density, particularly at the centre of the metal, which underscores covalent and electrostatic interactions. In this redistribution, the complex is stabilised, and the electronic communication between the metal ion and the ligand is improved [29].



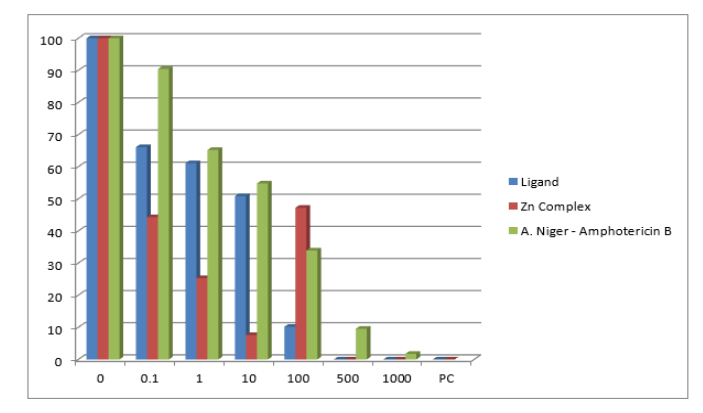
[Fig.7c: Total SCF Density of Ligand and its Metal Complex]

V. ANTIMICROBIAL ACTIVITIES

Antimicrobial activity of the oxime ligand, (benzoylamino)-3-sulfanylpropanoic acid and the Zn (II) complex were evaluated in vitro using the Minimum Inhibitory Concentration (MIC) method, both against Escherichia coli (MTCC-452) and Aspergillus niger (MTCC-281) [30]. The reference drugs used were ciprofloxacin and Amphotericin B, used for antibacterial and antifungal activity, respectively. As a ligand, it exhibited impressive antimicrobial activity, with MIC values of 100 μ g/mL and 0.06 μ g/mL, respectively, against *E. coli* and *A.* niger. When the coordination with Zn (II) was done, the complex was much more active, and the values of MIC against E. coli and A. niger were 1 µM and 0.04 2g/mL, respectively [31]. This has been improved by the augmented lipophilicity and chelation effect, which enable red meat to penetrate cell membranes better. Zn (II) complex was additionally found to be more effective than ciprofloxacin in antibacterial activity, and Amphotericin B, shown in Fig. 8a & 8b, in antifungal activity [32]. The activity rankings of Zn (II) complex were Ciprofloxacin and Ligand versus E. coli, and Zn (II) complex versus Ciprofloxacin and Amphotericin B versus A. niger. Such findings raise the issue of the synergistic nature of metal coordination shown in Table 5, which places the Zn (II) complex as a potential broadspectrum antimicrobial agent [33].



[Fig.8a: Antibacterial Activities (MIC Values) of Ligand and Metal Complex]



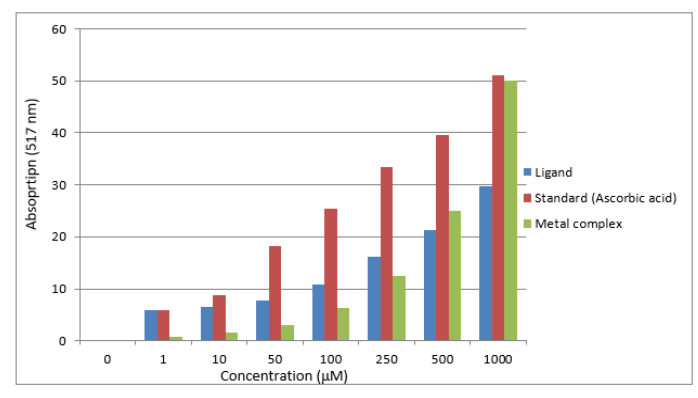
[Fig.8b: Antifungal Activities (MIC Values) of Ligand and Metal Complex]

Table V: Antimicrobial Activities of Ligand & its Metal Complex

S. No.	Compounds	Bacterial Strain <i>E. coli</i> MIC (μg/ml)	Fungal Strain A.niger MIC (µg/ml)	
1	Ligand	100 μg/mL	0.06 μg/mL	
2	Complex	1μmL	0.04µg/mL	
3	Ciprofloxacin	5μg/mL	=	
4	Amphotericin B	-	0.5μg/mL	

A. Antioxidant Properties

The DPPH radical scavenging assay was used to determine the antioxidant activity of the ligand and Zn (II) complex [34]. Under this technique, 10 µL of each test sample (1-1000 µM) was added to 0.2 mL of 0.1 mM DPPH solution in methanol in a 96-well plate. The mixtures were left to incubate in the dark, after which the absorbance at 517nm was measured with a microplate reader. The standard antioxidant was ascorbic acid [35]. The percentage inhibition was interpreted against the control, and the IC50 was determined using GraphPad Prism 6. The experiments indicated that there was a concentration-dependent radical scavenging activity in the ligand and Zn (II) complex shown in fig-7. The Zn (II) complex was more antioxidant compared to the free ligand. The IC50 of ascorbic acid was $27.17 \pm 0.006 \mu M$, and the approximate IC₅₀ of the ligand and Zn (II) complex were $^{\sim}550~\mu M$ and $^{\sim}420~\mu M$, respectively. This augmentation of the complexation implies that the complexation with Zn (II) enhances the free radical scavenging ability of this ligand [36].



[Fig.8c: Antioxidant Properties of Ligand and Metal Complex]



VI. MOLECULAR DOCKING

The binding interactions between 2 2-benzoylamino-3sulfanylpropanoic acid and its Zn (II) complex and the selected target proteins were analyzed by using AutoDock Vina [37]. The optimisation of the structures was performed using the Gaussian program, and objects were visualised with Gauss View. The file preparation for docking was completed using the Open Babel GUI. Three objectives of the docking simulations involved three proteins, viz., an antioxidant protein (PDB: 1HD2), an antimicrobial protein (PDB: 1D6N), and an enzyme inhibition protein (PDB: 1E66) [38]. Table 6 presents the outcomes of the data, including binding energy, electrostatic interaction, inhibitory constant, and thermodynamic constant. The pattern of interaction is depicted as a 3D micelle in Fig. 9a and as 3D ribbon models in Fig. 9 b. The affinity and strength of interaction of all the proteins with the Zn (II) complex were better than those of the free ligand with respect to the biochemical potential due to the metal coordination. Such a comprehensive study of docking determines the increased relevance of therapy of the Zn (II) complex [39].

A. Antioxidant Protein (PDB-1HD2) Interaction

The docking parameters show that the ligand, 2-(benzoylamino)-3-sulfanylpropanoic acid and Zn (II) complex had different interactions with antioxidant proteins. The binding energy of the Zn (II) complex (-4.87 kcal/mol) was marginally lower than that of the ligand (-5.86 kcal/mol), and so there was a slight decrease in affinity with complexation. Also, the inhibitory constant (15.07 µM in the case of the Zn (II) complex, as compared to 397.13 µM in the case of the ligand) indicates better inhibitory activity of the metal complex. The electrostatic energy was not significant in either system, suggesting that there were minimal polar interactions. Increased hydrophobicity and lipophilicity, when coordinated with metals, are reflected in the partition constant (151.70 kcal/mol of the complex). In general, the interaction of the Zn (II) complex with protein was more stable, which highlights the possibility of improving the antioxidant activity [40].

B. Antimicrobial Protein (PDB-1D6N) Interaction

Antimicrobial protein docking demonstrated the better binding of Zn (II) complex than that of the free ligand, as shown by a substantial decrease in binding energy (-8.70 kcal/mol and -5.16 kcal/mol, respectively) [41]. This tendency was also supported by the inhibitory constant, where the Zn (II) complex exhibited significantly stronger inhibitory power (421.51 µM compared to 202.72 µM for the ligand). The intermolecular energy of the complex (-11.68 kcal/mol) was also significantly smaller, and this indicates that there were stronger non-covalent forces. The electrostatic energy shift (+0.07 kcal/mol to the complex) suggests, however, the establishment of some small polar interactions that supplement the binding. These findings highlight the increased antimicrobial activity of the Zn (II) complex over the uncoordinated ligand [42].

C. Enzyme Inhibition (PDB-1E66) Interaction

In the enzyme inhibition studies, the Zn (II) complex was also found to be superior to the free ligand in terms of interaction profile [43]. The ligand had a stronger binding energy of -6.65 kcal/mol compared to the Zn (II) complex, which had a binding energy of -7.53 kcal/mol. The high inhibitory constant (138.25 µM of the complex vs 112.82 µM of the ligand) supports the fact that it can be a good enzyme inhibitor. The decrease in internal energy (-5.39 kcal/mol of the complex compared to -8.79 kcal/mol of the ligand) indicates a thermodynamically favourable binding reaction during the complexation process. The torsional free energy was, however, relatively similar, thus stating that the flexibility of the ligand was insignificantly influenced. The docking results support the increased potential of the Zn (II) complex in regulating the enzymatic activities [44].

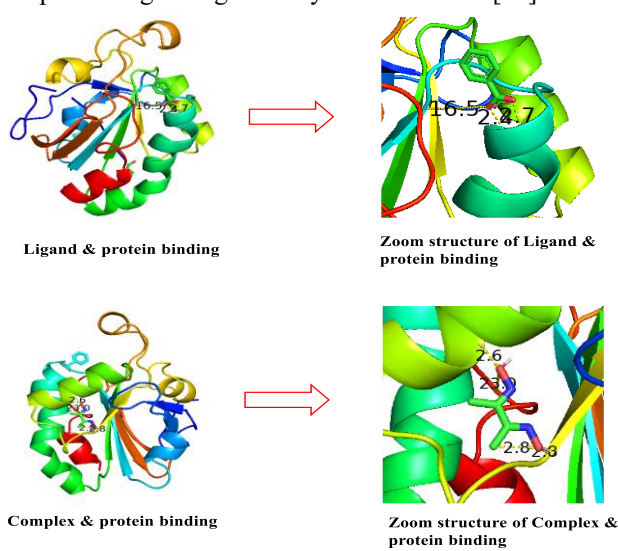


[Fig.9a: Ligand and Complex Interaction with Antioxidant Protein (PDB – 1HD2)]

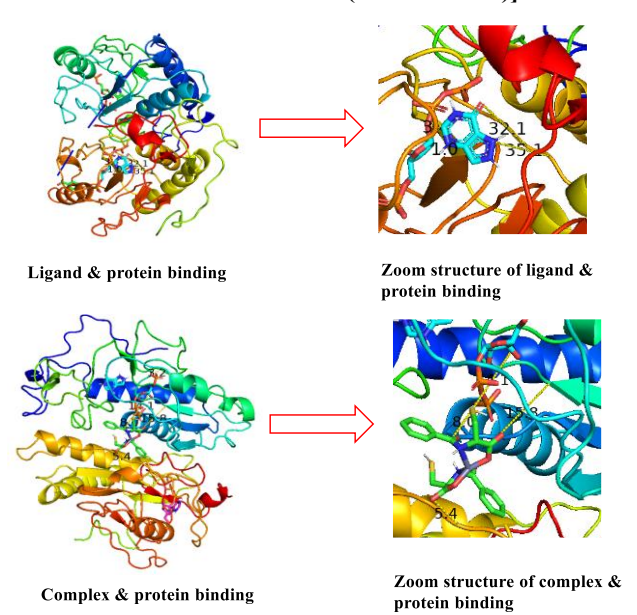


[Fig.9b: Ligand and Complex Interaction with Antimicrobial Protein (PDB-1D6N)]





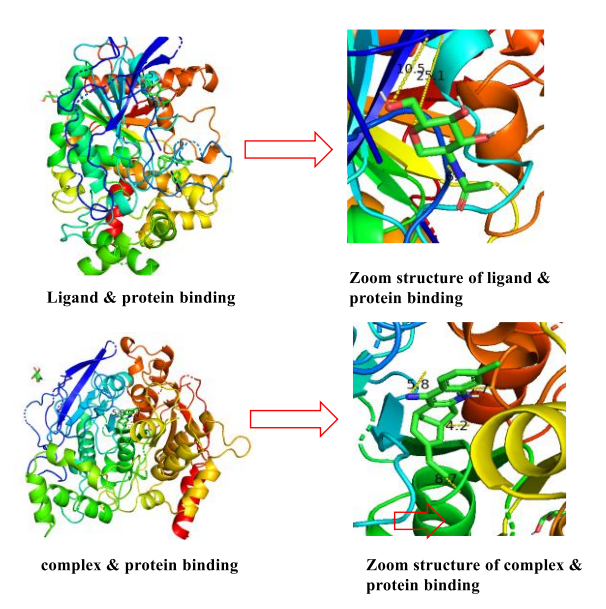


[Fig.9c: Ligand and Complex Interaction with Enzyme Inhibition (PDB-1E66)]
Table VI: Molecular Docking Results of Ligand & its Metal Complex

S. N	Chemical Properties	Ligand + Antioxidant Protein (PDB- 1HD2)	Zn (II) Complex + Antioxidant Protein (PDB- 1HD2)	Ligand+ Antimicrobial Protein (PDB-1D6N)	Zn (II) Complex + Antimicrobial Protein (PDB- 1D6N)	Ligand + Enzyme Inhibition (PDB- 1E66)	Zn (II) Complex Enzyme Inhibition (PDB- 1E66)
1	Grid energy	-5.86 Kcal/mol	-4.87 Kcal/mol	-5.16 Kcal/mol	-8.70 Kcal/mol	-7.80 Kcal/mol	-6.90 Kcal/mol
2	Binding Energy (Kcal/mol)	1.789 Kcal/mol	1.1932Kcal/mol	-5.04 Kcal/mol	-8.70 Kcal/mol	-6.65 Kcal/mol	-7.53 Kcal/mol
3	Electrostatic energy	-0.17Kcal/ mol	0.00Kcal/ mol	-0.08 Kcal/mol	0.07 Kcal/mol	0.07Kcal/mol	-0.31 Kcal/mol
4	Inhibitory constant	397.13μm	15.07µm	202.72μm	421.51μm	112.82µm	138.25μm
5	Partition constant(Q)	50.34Kcal/mol	151.70 Kcal/mol	50.41 Kcal/mol	50.52 Kcal/mol	50.75 Kcal/mol	50.46 Kcal/mol
6	Free energy (A)	-2321.84K cal/mol	-2975.37 Kcal/mol	-2322.64 Kcal/mol	-2323.93 Kcal/mol	-2326.59 Kcal/mol	-2323.19 Kcal/mol
7	Internal energy(U)	4.04 Kcal/mol	-6.66 Kcal/mol	-4.84 Kcal/mol	-6.13 Kcal/mol	-8.79 Kcal/mol	-5.39 Kcal/mol
8	Entropy (S)	7.77 Kcal/mol	9.96 Kcal/mol	7.77 Kcal/mol	7.77 Kcal/mol	7.77 Kcal/mol	7.77 Kcal/mol
9	Torsional free energy	1.79 Kcal/mol	1.19 Kcal/mol	-7.72 Kcal/mol	2.98 Kcal/mol	2.98 Kcal/mol	1.79 Kcal/mol
10	Intermolecular energy	-6.43 Kcal/mol	-7.77 Kcal/mol	-7.72 Kcal/mol	-11.68 Kcal/mol	-12.46 Kcal/mol	-8.51 Kcal/mol
11	Unbound system energy	-15.3 Kcal/mol	-2.47 Kcal/mol	1.79 Kcal/mol	-3.77 Kcal/mol	-2.93 Kcal/mol	-0.67 Kcal/mol
12	Grid dimension	31.220, 65.132, 43.442	31.593, 66.257, 43.817	29.095, 90.037, 79.938,	75.222, 65.173, 34.021,	29.610, 88.393, 85.835,	71.566, 55.277, 34.021
13	Grid spacing	0.375Å	0.375Å	0.375Å	0.375Å	0.375Å	0.375Å

VII. ANTICANCER PROPERTIES

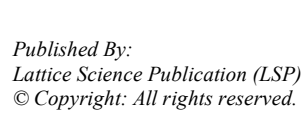
The cytotoxic effect of the ligand and the complex between ligand and Zn (II) was examined using MTT assay on the human breast cancer cell line, MCF-7. Cells of MCF-7 (10,000 cells/well) were grown in 96-well plates in the presence of DMEM medium with 10% fetal bovine serum and 1% penicillin-streptomycin and allowed to incubate at 37°C in a 5% CO₂ environment. The following occurs after 24 hours, during which the cells were exposed to different concentrations of the ligand and its metal complex, prepared in DMSO and diluted in an incomplete medium, as shown in Fig. 10. Control wells had untreated cells, and blank wells did not contain MTT. The MTT solution (5mg/mL) was added after 24 hours of exposure and incubated for 2 hours.

Crystal growth of viable cells was malformed by using DMSO, and absorbance was measured at 540 nm. The determination of IC₅₀ was done in GraphPad Prism 6, and the results were presented as mean and Standard error of the mean. Morphological observation was done under an inverted microscope. The Zn (II) complex exhibited greater cytotoxicity than the free ligand, with a reduced IC₅₀. This indicates a higher anticancer potential due to the coordination of the metals, which could be attributed to increased cellular uptake or reactivity. Therefore, the Zn (II) complex can be used as a promising anticancer drug

entuol neibn

development candidate in the

future [45].



Synthesis, Spectroscopic Characterizations, Antimicrobial, Anticancer & Anitoxidant Activities, Molecular Docking and DFT Calculations of Noval Zinc (II) Complex of 2-(Benzoylamino)-3-Sulfanylpropanoic Acid

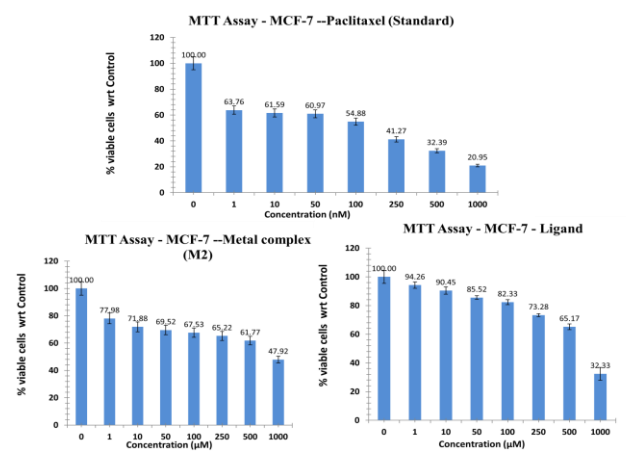


[Fig.10: Anticancer Activities (MIC Values) of Ligand and Metal Complex]

VIII. CONCLUSION

The paper has been able to synthesize and describe a zinc (II) complex of 2- (benzoylamino)-3-sulfanylpropanoic acid using a combination of spectroscopic, analytical and computational methods. The FT-IR, UV-visible spectroscopy, mass spectrometry, ¹H NMR, and ¹³C NMR data were used to verify the structural integrity of this complex, and SEM and powder XRD were used to determine the morphology and crystalline structure. The DFT computations of the structure, electrons and stability of the complex demonstrated the effect of zinc coordination on the chemical characteristics of the complex. Biological measurements indicated that the zinc (II) complex exhibited a better antimicrobial effect than the free ligand and the conventional drugs. The zinc (II) complex had the best antibacterial activity against E. coli, when compared to Ciprofloxacin and the free ligand. On the same note, its antifungal effect on A.niger was more pronounced than on the ligand and Amphotericin B. The antioxidant activity of the Zn (II) complex in the DPPH test was greater than that of the free ligand, with a lower IC50 (\sim 420 μM vs. \sim 550 μM), reflecting a favourable radical scavenging potential when metals coordinate the ligand. The molecular docking experiments revealed good interactions between the zinc (II) complex and antioxidant, antimicrobial, and enzyme inhibition proteins, making it suitable for use in targeted therapy applications. The increase in the bioactivity of the zinc (II) complex is explained by the electronic and structural changes introduced by metal coordination, allowing it to interact more strongly with the biological target. Moreover, cytotoxicity tests on the MCF-7 cell line of breast cancer demonstrated that the Zn (II) complex exhibited significantly greater anticancer activity than the free ligand, as indicated by the lower IC₅₀ value in the MTT assay. These observations point to the development of the Zn (II) complex as a good candidate for future pharmacological/biochemical studies.

ACKNOWLEDGMENTS

The Authors are thankful to the Nanoscience Department of Chemistry, DSB Campus, Nainital, University of Delhi, India, for providing analytical facilities and cooperating in recording the spectra of the synthesised compounds, and to Aakaar Biotechnologies Private Limited, Lucknow (India), for conducting the antimicrobial study.

DECLARATION STATEMENT

After aggregating input from all authors, I must verify the accuracy of the following information as the article's author.

- Conflicts of Interest/ Competing Interests: Based on my understanding, this article has no conflicts of interest.
- Funding Support: This article has not been funded by any organizations or agencies. This independence ensures that the research is conducted with objectivity and without any external influence.
- Ethical Approval and Consent to Participate: The content of this article does not necessitate ethical approval or consent to participate with supporting documentation.
- Data Access Statement and Material Availability: The adequate resources of this article are publicly accessible.
- Author's Contributions: The authorship of this article is contributed equally to all participating individuals.

REFERENCES

- H.R. Sonawane, B.T. Vibhute, B.D. Aghav, J.V. Deore, S.K. Patil, Versatile applications of transition metal incorporating quinoline Schiff base metal complexes: An overview, Eur. J. Med. Chem. 258 (2023) 115549. DOI: https://doi.org/10.1016/j.ejmech.2023.115549.
- S.F. Kainat, M.B. Hawsawi, E.U. Mughal, N. Naeem, A.M. Almohyawi, H.M. Altass, E.M. Hussein, A. Sadiq, Z. Moussa, A.S. Abd-El-Aziz, Recent developments in the synthesis and applications of terpyridine-based metal complexes: a systematic review, RSC Adv. 14 (2024) 21464–21537.
 DOI: https://doi.org/10.1039/D4RA04119D.
- Z. Kazemi, N. Moini, H.A. Rudbari, N. Micale, A comprehensive review on the development of chiral Cu, Ni, and Zn complexes as pharmaceutical agents over the past decades: Synthesis, molecular structure and biological activity, Med. Res. Rev. (2024) med.22083. DOI: https://doi.org/10.1002/med.22083.
- M. Biswas, K.K. Choudhury, A. Banerjee, R.K. Pathak, Elevating the discourse on drug delivery: A fresh perspective on the utilisation of coordination chemistry-driven metal-drug conjugates, Coord. Chem. Rev. 517 (2024) 216026.
 DOI: https://doi.org/10.1016/j.ccr.2024.216026.
- L. Li, C. Ma, Y. Yang, B. Wang, X. Liu, Y. Wang, X. Bian, G. Zhang, N. Zhang, Exploring the Potential of Plant-Derived Metal Ion Binding Peptides: Preparation, Structure-Activity Relationship, and Biological Activities, Trends Food Sci. Technol. (2024) 104650. DOI: https://doi.org/10.1016/j.tifs.2024.104650.
- P. Marinova, K. Tamahkyarova, Synthesis and Biological Activities of Some Metal Complexes of Peptides: A Review, BioTech 13 (2024) 9. DOI: https://doi.org/10.3390/biotech13020009.
- S.S. Ibrahim, M.Y. Al-darwesh, S.W. Arkawazi, K.A. Babakr, I.N. QADER, Synthesis, Characterization, Antioxidant, Antibacterial Activity, and Molecular Docking Studies of Zn (II) and Cu (II) Complexes Nanoparticles, J. Mol. Struct. (2024) 141120.
 DOI: https://doi.org/10.1016/j.molstruc.2024.141120.
- Z. Razmara, P. Karimi, E. Parisi, Single crystal structure features, optimization of ultrasonic conditions, density functional theory studies, and antibacterial activity of a new organic compound, J. Mol. Struct. 1322 (2025) 140437.
 DOI: https://doi.org/10.1016/j.molstruc.2024.140437.
- X. Zhao, J. Wei, T. Song, Z. Wang, D. Yang, X. Zhang, F. Huo, Y. Zhang, H.-M. Xiong, Computational insights into carbon dots: Evolution of structural models and structure–activity relationships, Chem. Eng. J. (2024) 148779.





- DOI: https://doi.org/10.1016/j.cej.2024.148779.
- S. Sakthiveni, A. Xavier, M. Tamilelakkiya, R. Sakthivadivel, P. Suguna, P. Pandi, P. Velusamy, S.E. Muthu, K.A. Kumar, Synthesis and characterization of novel Schiff base ligands and their Cu (II), Zn (II), Co (II), and Ni (II) complexes: DNA binding, antibacterial activity, and docking studies, J. Mol. Struct. (2024) 141000.
 DOI: https://doi.org/10.1016/j.molstruc.2024.141000.
- M. Ajmal, A.K. Mahato, M. Khan, S. Rawat, A. Husain, E.B. Almalki, M.A. Alzahrani, A. Haque, M.J.M. Hakme, A.S. Albalawi, M. Rashid, Significance of Triazole in Medicinal Chemistry: Advancement in Drug Design, Reward and Biological Activity, Chem. Biodivers. 21 (2024) e202400637.
 DOI: https://doi.org/10.1002/cbdv.202400637.
- A. Kumar, S. Ahmed, M. Bhardwaj, S. Imtiaz, D. Kumar, A.R. Bhat, B. Sood, S. Maji, In vitro Anti-microbial, DNA-binding, In silico Pharmacokinetics and Molecular Docking Studies of Schiff-based Cu (II), Zn (II) and Pd (II) Complexes, J. Mol. Struct. (2024) 138695. DOI: https://doi.org/10.1016/j.molstruc.2024.138695.
- H. Kargar, M. Fallah-Mehrjardi, K.S. Munawar, Metal complexes incorporating tridentate ONO pyridyl hydrazone Schiff base ligands: Crystal structure, characterization and applications, Coord. Chem. Rev. 501 (2024) 215587.
 DOI: https://doi.org/10.1016/j.ccr.2023.215587.
- A.A. Mohamed, S.A. Sadeek, N.G. Rashid, H.S. Elshafie, I. Camele, Synthesis, Characterization and Evaluation of the Antimicrobial and Herbicidal Activities of Some Transition Metal Ions Complexes with the Tranexamic Acid, Chem. Biodivers. 21 (2024) e202301970. DOI: https://doi.org/10.1002/cbdv.202301970.
- S. Maity, S. Kolay, S. Chakraborty, A. Devi, A. Patra, A. comprehensive review of atomically precise metal nanoclusters with emergent photophysical properties towards diverse applications, Chem. Soc. Rev. (2025). DOI: https://doi.org/10.1039/D4CS00962B.
- A. Schultheiss, J. White, K. Le, N. Boone, U. Riaz, D.K. Taylor, The Synthesis, Characterization, and Theoretical Study of Ruthenium (II) Polypyridyl Oligomer Hybrid Structures with Reduced Graphene Oxide for Enhanced Optoelectronic Applications, Int. J. Mol. Sci. 25 (2024) 12989. DOI: https://doi.org/10.3390/ijms252312989.
- T. Salah, A.B. Ahmed, N. Krayem, A. Guesmi, N.B. Hamadi, L. Khezami, H. Naïli, B. Hamdi, Two different coordination polyhedra in the crystal structure of a novel Zn (II) hybrid complex: DFT investigation, biological activities and emission properties, J. Mol. Struct. 1296 (2024) 136863.
 DOI: https://doi.org/10.1016/j.molstruc.2023.136863.
- J. Żygowska, M. Orlikowska, I. Zhukov, W. Bal, A. Szymańska, Copper interaction with cystatin C: effects on protein structure and oligomerization, FEBS J. 291 (2024) 1974–1991.
 DOI: https://doi.org/10.1111/febs.17092.
- R. Rajamohan, P. Muthuraja, S. Ashokkumar, M. Muralikrishnan, K. Murugavel, C. Govindasamy, Y.R. Lee, A non-toxic inclusion complexation of loxoprofen with hydroxypropyl-β-cyclodextrin for complete solubility and anti-inflammatory efficacy, J. Mol. Liq. 410 (2024) 125612. DOI: https://doi.org/10.1016/j.molliq.2024.125612.
- L. Chen, L. Wang, L. Ma, C. Wang, X. Qin, M. Wang, X. Zhang, R. Yang, B. Fang, J. An, Synergistic Antioxidant Effects of Cysteine Derivative and Sm-Cluster for Food Applications, Antioxidants 13 (2024) 910. DOI: https://doi.org/10.3390/antiox13080910.
- S. Shaaban, K.T. Abdullah, K. Shalabi, T.A. Yousef, O.K. Al Duaij, G.M. Alsulaim, H.A. Althikrallah, M. Alaasar, A.S.M. Al-Janabi, A.M. Abu-Dief, Synthesis, Structural Characterization, Anticancer, Antimicrobial, Antioxidant, and Computational Assessments of Zinc(II), Iron(II), and Copper(II) Chelates Derived From Selenated Schiff Base, Appl. Organomet. Chem. 38 (2024) e7712. DOI: https://doi.org/10.1002/aoc.7712.
- O. Hakami, A.M.A. Alaghaz, T. Zelai, S.A.H. Albohy, Bio-evaluation of pyrazolone-furan derived Schiff base Cr(III), Co(II), Ni(II), Cu(II), and Zn(II) nano-sized complexes: Design, spectral characterization, antimicrobial efficacy, antioxidant activity, apoptotic activity, and cell cycle analysis, Appl. Organomet. Chem. 38 (2024) e7488. DOI: https://doi.org/10.1002/aoc.7488.
- A. Aguilar Garrido, Waste-derived Technosols for the treatment of soil and water affected by potentially harmful elements, PhD Thesis, Universidad de Granada, 2024. https://digibug.ugr.es/bitstream/handle/10481/94671/93363.pdf?sequence=4&isAllowed=y (accessed December 28, 2024).
- 24. A. Das, S.A. Hussain, H. Banik, D. Maiti, T. Aktar, B. Paul, P. Debnath, L. Sieroń, A. Bhattacharya, K.L. Bhowmik, Cd (II) and Zn (II) complexes with 2-mercaptopyridine: Synthesis, crystal structure, Hirshfeld surface analysis, luminescent properties, aggregation behaviours, current-voltage characteristic and antibacterial assay, Polyhedron 247 (2024) 116747.

- DOI: https://doi.org/10.1016/j.poly.2023.11674.
- Z. Li, M. Chen, W. Zhu, R. Xin, J. Yang, S. Hu, J. You, D.Y. Ryu, S.-H. Lim, S. Li, Advances and perspectives of composite nanoarchitectonics of nanocellulose/metal-organic frameworks for effective removal of volatile organic compounds, Coord. Chem. Rev. 520 (2024) 216124. DOI: https://doi.org/10.1016/j.ccr.2024.216124,
- H.M. Abd El-Lateef, A.M. Ali, M.M. Khalaf, A. Abdou, New Fe (III), Co (II), Ni (II), Cu (II), and Zn (II) mixed-ligand complexes: strucMorocco, DFT, biological, and molecular docking studies, Bull. Chem. Soc. Ethiop. 38 (2024) 397–416.
 DOI: https://doi.org/10.4314/bcse.v38i2.9.
- S. Singh, M. Choudhary, Synthesis of Zn (ii) coordination complexes, their molecular design and docking with SARS-CoV-2 RBD protein and Omicron spike protein, New J. Chem. 48 (2024) 9287–9313. DOI: https://doi.org/10.1039/D3NJ04714H.
- A.I. Osman, A. Ayati, P. Krivoshapkin, B. Tanhaei, M. Farghali, P.-S. Yap, A. Abdelhaleem, Coordination-driven innovations in low-energy catalytic processes: advancing sustainability in chemical production, Coord. Chem. Rev. 514 (2024) 215900.
 DOI: https://doi.org/10.1016/j.ccr.2024.215900.
- K. Manogaran, T. Sivaranjani, P. Sengeny, V.S.K. Venkatachalapathy, M. Mahadevan, K. Elangovan, S. Armaković, S.J. Armaković, B.F. Abramović, Investigation on molecular and biomolecular spectroscopy of the novel 2BCA molecule to analyse its biological activities and binding interaction with Nipah viral protein, Spectrochim. Acta. A. Mol. Biomol. Spectrosc. 321 (2024) 124737. DOI: https://doi.org/10.1016/j.saa.2024.124737.
- S. Haddou, K. Mounime, E. Loukili, D. Ou-Yahia, A. Hbika, M.Y. Idrissi, A. Legssyer, H. Lgaz, A. Asehraou, R. Touzani, Investigating the Biological Activities of Moroccan Cannabis Sativa L Seed Extracts: Antimicrobial, Anti-inflammatory, and Antioxidant Effects with Molecular Docking Analysis, Morocco. J. Chem. 11 (2023) 11–4. DOI: https://doi.org/10.48317/IMIST.PRSM/morjchem-v11i04.42100.
- I.S. Sow, M. Gelbcke, F. Meyer, M. Vandeput, M. Marloye, S. Basov, M.J. Van Bael, G. Berger, K. Robeyns, S. Hermans, D. Yang, V. Fontaine, F. Dufrasne, Synthesis and biological activity of iron(II), iron(III), nickel(II), copper(II) and zinc(II) complexes of aliphatic hydroxamic acids, J. Coord. Chem. 76 (2023) 76–105. DOI: https://doi.org/10.1080/00958972.2023.2166407.
- R. Chand, M. Ahmed, B.K. Singh, A Review: Recent Advances in Chemistry and Applications of 2, 4-Dihydroxybenzaldehyde Oxime and Its Transition Metal Complexes, J. Adv. Chem. Sci. (2024) 808– 812. DOI: https://doi.org/10.30799/jacs.264.24100401.
- K.M. Ismail, F.B. Rashidi, S.S. Hassan, Ultrasonic synthesis, characterization, DFT and molecular docking of a biocompatible Zn-based MOF as a potential antimicrobial, anti-inflammatory and antitumor agent, Sci. Rep. 14 (2024) 21989.
 DOI: https://www.nature.com/articles/s41598-024-71609-7#citeas
- 34. S. Shaaban, K.T. Abdullah, K. Shalabi, T.A. Yousef, O.K. Al Duaij, G.M. Alsulaim, H.A. Althikrallah, M. Alaasar, A.S.M. Al-Janabi, A.M. Abu-Dief, Synthesis, Structural Characterization, Anticancer, Antimicrobial, Antioxidant, and Computational Assessments of Zinc(II), Iron(II), and Copper(II) Chelates Derived From Selenated Schiff Base, Appl. Organomet. Chem. 38 (2024) e7712.
 DOI: https://doi.org/10.1002/aoc.7712.
- X. Chen, G. Chen, M. Li, Z. Liu, W. Dai, F. Wang, H. Zhang, F. Liu,
 Y. Zhu, Structural characterization, biological activities, and rheological behavior of an exopolysaccharide from tea-bacteria Herbaspirillum sp. S-1, Carbohydr. Polym. Technol. Appl. (2025) 100842. DOI: https://doi.org/10.1016/j.carpta.2025.100842.
- E.M. Abdalla, S.A. Aly, Using Coordination Compounds as Antioxidants, in: Power Antioxid.-Unleashing Nat. Def. Oxidative Stress, IntechOpen, 2025. https://www.intechopen.com/chapters/1186865 (accessed May 30, 2025). DOI: https://doi.org/10.5772/intechopen.1005817
- Y. Min, Y. Wei, P. Wang, X. Wang, H. Li, N. Wu, S. Bauer, S. Zheng, Y. Shi, Y. Wang, J. Wu, D. Zhao, J. Zeng, From Static to Dynamic Structures: Improving Binding Affinity Prediction with Graph-Based Deep Learning, Adv. Sci. 11 (2024) 2405404.
 DOI: https://doi.org/10.1002/advs.202405404.
- M.D. Rahman, G.J. Quadri, B. Doppalapudi, D.A. Szafir, P. Rosen, A qualitative analysis of standard practices in annotations: A taxonomy and design space, IEEE Trans. Vis. Comput. Graph. (2024).



Synthesis, Spectroscopic Characterizations, Antimicrobial, Anticancer & Anitoxidant Activities, Molecular Docking and DFT Calculations of Noval Zinc (II) Complex of 2-(Benzoylamino)-3-Sulfanylpropanoic Acid

DOI: https://doi.org/10.1109/TVCG.2024.3456359.

- P. Taweechat, P. Boonamnaj, M. Samsó, P. Sompornpisut, Significance of Zn²⁺ in RyR1 for Structural Integrity and Ligand Binding: Insight from Molecular Dynamics, J. Phys. Chem. B 128 (2024) 4670–4684. DOI: https://doi.org/10.1021/acs.jpcb.4c01189.
- H.M. Abd El-Lateef, M.M. Khalaf, A. Abdou, Exploring the molecular structure and in vitro biological potential of newly synthesised Fe (III), Co (II), and Ni (II) coordination compounds with 2-(pyridin-2-yl)-1H-benzimidazole and phenylalanine ligands, Polyhedron (2024) 117103.

DOI: https://doi.org/10.1016/j.poly.2024.117103.

- M.S.A. Mansour, A.T. Abd-Elkarim, A.A. El-Sherif, W.H. Mahmoud, Manganese, cobalt, and cadmium complexes of quinazoline schiff base ligand and methionine: synthesis, characterization, DFT, docking studies and biomedical application, Egypt. J. Chem. 67 (2024) 479–506.
 DOI: https://dx.doi.org/10.21608/ejchem.2024.266673.9275.
- O. Danilescu, P. Bourosh, I. Bulhac, S. Shova, V.C. Kravtsov, M.N. Caraba, I.V. Caraba, R. Popescu, M. Crisan, D. Haidu, Laminated dihydrazone Zn (II) coordination polymer with prospects for sensory and multifunctional biomedical applications, Polyhedron 258 (2024) 117039. DOI: https://doi.org/10.1016/j.poly.2024.117039.
- T. Salah, A.B. Ahmed, N. Krayem, A. Guesmi, N.B. Hamadi, L. Khezami, H. Naïli, B. Hamdi, Two different coordination polyhedra in the crystal structure of a novel Zn (II) hybrid complex: DFT investigation, biological activities and emission properties, J. Mol. Struct. 1296 (2024) 136863.

DOI: https://doi.org/10.1016/j.molstruc.2023.136863

- H.M. Abd El-Lateef, A.M. Ali, M.M. Khalaf, A. Abdou, New iron (III), cobalt (II), nickel (II), copper (II), zinc (II) mixed-ligand complexes: Synthesis, structural, DFT, molecular docking and antimicrobial analysis, Bull. Chem. Soc. Ethiop. 38 (2024) 147–166. DOI: https://doi.org/10.4314/bcse.v38i1.12.
- 45. Tihauan, Bianca & Berca, Lavinia & Adascălului, Marian & Sanmartin, Angel & Nica, Silvia &Cimponeriu, Danut & Duta, Denisa. (2020). Experimental in vitro cytotoxicity evaluation of plant bioactive compounds and phytoagents: a review. Romanian Biotechnological Letters. 25. 1832-1842.

DOI: https://doi.org/10.25083/rbl/25.4/1832.1842.

AUTHOR'S PROFILE



Mohseen Ahmed is a research scholar in the Department of Chemistry at M.B. Government Post-Graduate College, Haldwani (Nainital), is affiliated with Kumaun University. Nainital. He is pursuing a PhD in Chemistry with a focus on Organometallic Chemistry. He holds an M.Sc. in Organic Chemistry (2018) and a B.Sc. in PCM

(2016) from Kumaun University. With over eight years of teaching experience at various reputed institutions and online platforms, he has guided students from school to postgraduate levels. His research work has been published in reputed journals such as the Journal of Coordination Chemistry and the Journal of Advanced Chemical Sciences. He has qualified for MP SET (2023), GATE (2024), and CSIR-UGC NET (2024-2025) and actively participates in national and international conferences and workshops related to advanced chemical science.



Reema Chand is a research scholar in the Department of Chemistry at M.B. Government Post-Graduate College, Haldwani (Nainital), affiliated with Kumaun University, Nainital. She is currently pursuing her Ph.D. in Chemistry with a specialization in Organometallic Chemistry. She completed her M.Sc. in Organic Chemistry (2018) and

B.Sc. in PCM (2016) from Kumaun University. With over four years of teaching experience, she has guided students of both undergraduate and postgraduate levels at the reputed institution Haldwani. She has qualified U-SET (2023) and has soualified U-SET 2023) and has several research publications in reputed journals such as the Journal of Coordination Chemistry and Journal of Advanced Chemical Sciences. She has actively participated in numerous national and international conferences and workshops related to chemistry, analytical techniques, and artificial intelligence applications in chemical sciences.



Prof. Bibhesh K Singh has done M.Sc. and PhD (Chemistry) from the University of Delhi. He has been engaged in teaching, research, and various administrative work for the last 27 years. He has published nearly 50 research papers, mainly in journals such as Elsevier, Springer, and Taylor Francis. He has completed five

research projects funded by CSIR and UGC and supervised six research

students for PhD courses. Presently works as Principal for the last six years in the Department of Higher Education, Govt of Uttarakhand.

Disclaimer/Publisher's Note: The statements, opinions and data contained in all publications are solely those of the individual author(s) and contributor(s) and not of the Lattice Science Publication (LSP)/ journal and/ or the editor(s). The Lattice Science Publication (LSP)/ journal and/or the editor(s) disclaim responsibility for any injury to people or property resulting from any ideas, methods, instructions or products referred to in the content.

